Journal of Low Temperature Physics, Vol. 49, Nos. 3/4, 1982

Inhomogeneous Nucleation of Superfluid Vorticity at a Sharp Edge*

Yorke J. Brown

Department of Physics, Applied Physics and Astronomy, State University of New York at Binghamton, Binghamton, New York

George B. Hess

Department of Physics, University of Virginia, Charlottesville, Virginia

(Received March 22, 1982)

We report an experiment in which superfluid flow through a single 10-μm diameter orifice is examined at pressure heads as low as 0.03 dyne/cm^2. Accurate measurements of low pressure head are made possible by a recirculating flow cryostat, capable of generating a calibrated, continuous flow of superfluid helium. Current vs. potential data for temperatures between 1.46 and 2.14 K are analyzed according to the Iordanskii–Langer–Fisher thermal nucleation theory, modified to apply to a model in which vortex half-rings are inhomogeneously nucleated at the sharp-edged mouth of the orifice. We offer two possible interpretations of the results.

1. INTRODUCTION

The homogeneous nucleation theory originally due to Iordanskii[1] and to Langer and Fisher[2] (ILF) explains in an elegant way how free vortex rings created by random thermal fluctuations can extract energy from the flow of superfluid helium. When a thermally nucleated vortex ring expands to the size of the flow channel, it annihilates a wavelength of the phase of the superfluid wave function, thus decelerating the fluid. In an isothermal flow experiment in which the flow velocity v_s is maintained constant, the pressure head Δp required to maintain steady flow is proportional to the frequency ν of production of "critical vortices"—those that can successfully cross the channel and contribute to dissipation. The vortex production frequency is, in turn, proportional to a Boltzmann factor relating to the

*Parts of this work were carried out with the support of National Science Foundation grants DMR-72-02971 and DMR-78-10778.

0022-2291/82/1100-0267$03.00/0

probability for finding the fluid in a flow state containing a critical vortex. Explicitly, the pressure head due to thermally nucleated vortices is[3]

$$\Delta p = \rho \kappa V \nu_0 \exp\left[-E_a(v_s)/kT\right] \tag{1}$$

where ρ is the fluid density, κ is the quantum of circulation, V is the volume available for nucleation, ν_0 is some attempt frequency per unit volume, and $E_a(v_s)$ is the activation energy, or the free energy required to create a critical vortex. The correct interpretation of the attempt frequency remains a serious problem with the ILF theory, but it has usually been identified with the atomic collision rate[2,3]—something like 10^{34} sec^{-1} cm^{-3}. Donnelly and Roberts[4] have calculated a similar value from the specific model of critical vortices nucleated as rotons.

In the original version of the ILF theory, the critical flow state was taken to consist of a free circular vortex ring whose self-induced velocity just holds it stationary in the flow. Since self-induced velocity depends upon the curvature of the filament, the critical vortex is identified by a critical radius R_c. Larger, slower rings will expand and contribute to dissipation; smaller, faster ones will contract and vanish. The energy of a free critical vortex ring is

$$E_a(v_s) = \beta(\rho_s/\rho)v_s^{-1} \tag{2}$$

where ρ_s is the superfluid density, and

$$\beta \equiv \rho\kappa^3(\eta - 1/2)(\eta - 5/2)/16\pi \tag{3}$$

Here, η is the vortex parameter defined by

$$\eta \equiv \ln(8R_c/a) \tag{4}$$

where a is the core radius. For most geometries, η is nearly constant and has a value of about three.

Several experimental investigations[3,5–10] have shown qualitative agreement with the ILF theory, but, in general, critical velocities are lower and temperature dependences are weaker than predicted. Most early experiments were performed in submicrometer-sized channels in order to suppress the various "extrinsic" dissipation mechanisms. One of the authors,[9] however, produced intrinsically limited flows in single 10-μm pinhole orifices by "guarding" the sample with rouge superleaks. This experiment showed substantially higher critical velocity and stronger temperature dependence than previous investigations, but still did not match the theory. In order to explain the remaining discrepancies, it was suggested that the vortices responsible for dissipation were being nucleated inhomogeneously in localized, high-velocity regions at the orifice lip or near irregularities in the channel wall. Since the local velocity determines the activation energy,

such a process would lower the critical velocity. Furthermore, these vortices would not be free rings, but would be truncated rings attached to the channel walls. Their lower energies would tend to bring down the critical velocity even further; but more importantly, velocity nonuniformities in the velocity-enhanced regions distort the shape of the critical vortex, ultimately resulting in altered temperature dependence of the critical velocity.

This paper reports an experiment which indicates that most of the dissipation in a pinhole of this type may be due to inhomogeneous nucleation of flattened half-rings attached to the orifice lip. The apparatus used in this investigation drives a continuous superflow through a 10-μm pinhole guarded with jeweller's rouge superleaks. The pressure head is measured with capacitive manometers sensitive to less than 0.03 dyne/cm^2, and since the continuous superflow permits integrating pressure heads over several minutes, the processes are assured of being in steady state, and full advantage is taken of the manometer sensitivity. By contrast, in a gravitational flow experiment with this type of orifice and typical reservoir cross sections ($\sim$1 cm^2), $dp/dt \approx 0.1$ dyne/cm^2 sec at low temperatures.

2. APPARATUS

The continuous superflow apparatus[11] is illustrated schematically in Fig. 1. Flow at a constant mass flux is maintained by a distillation pump similar to that used by van der Heijden *et al.*[12] The thermomechanical effect-draws fluid through the superleak SL into the heated evaporator tube. Vapor then passes through the exit orifice at the top of the evaporator and condenses in the surrounding condenser, which is cooled by close contact with the bath. A vacuum space insulates the evaporator and condenser from each other. The mass flux is fixed by the heat input to the evaporator, and the flow velocity is calculated from the mass flux and sample geometry. Film backflow is restricted by the small (1-mm-diameter) vapor exit orifice, but a calibrated correction was also applied to the data.

The flow circuit is completed through the sample channel by way of four "thermal valves,"[13] which can be used to shunt or reverse the flow. The shunting feature is particularly valuable because it provides a convenient, nondissiptative reference path.

A pair of capacitive manometers is used to measure the pressure difference across the sample. Each manometer is a vertically oriented coaxial capacitor into which fluid is admitted to vary its capacitance. The capacitance of each manometer tunes a tunnel diode oscillator so that a change in frequency of oscillation is proportional to a change in fluid level in the manometer. The difference frequency, corresponding to pressure

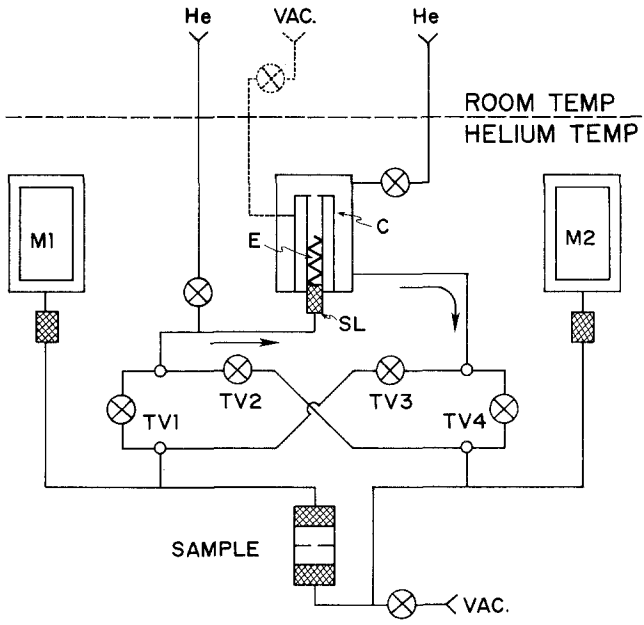

Fig. 1. Schematic of the continuous flow cryostat. Superfluid is drawn through the superleak SL into the heated evaporator tube E. Vapor from the evaporator passes to the condenser C, where it condenses and enters the flow circuit. Flow may be shorted or reversed by means of the four thermal valves TV1–4. Pressure head across the sample is measured by two capacitive manometers M1 and M2.

head, is obtained by mixing the two manometer signals with a doubly balanced diode mixer. The sensitivity of the manometers is about 4.7×10^{-3} cm/kHz, with noise of about ± 15 Hz. This corresponds to a resolution of less than 1 μm of liquid helium, or about 0.01 dyne/cm.[2]

The sample itself is a "utility optical pinhole" supplied by the Ealing Corp. It is a 3-mm-diameter nickel foil disk, 20 μm thick, with a single hole of 10 μm nominal diameter electroformed in the center. The particular orifice used in this work appears slightly elliptical when viewed under a microscope. Its axes are 9.9 and 8.8 ± 0.5 μm, making an open area of 6.8×10^{-7} cm.[2] The channel is flared on one side, as shown in Fig. 2a. Scanning electron micrographs of this orifice indicate that the angle between the inner surface of the channel and the surface of the plate (denoted by θ in Fig. 2) is about 90°. The radius of the lip is less than 0.05 μm. The micrographs also reveal the presence of numerous micrometer-sized, variously shaped bumps and indentations on the interior surface of the channel. The data reported here are all for flow from the flared side to the

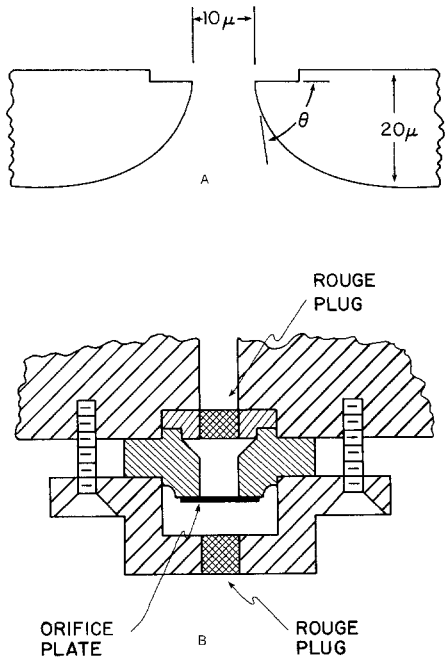

Fig. 2. The sample channel. (a) A cross section of the orifice. (b) Mounting of the orifice on a flange guarded by superleaks.

sharp-edged side, but spot checks in the opposite direction revealed similar behavior.

The orifice plate is cemented to a stainless steel sample mount, which in turn is bolted to the cryostat, as shown in Fig. 2b. Sealed to each side of the sample mount is a fitting with a 2-mm-diameter rouge-packed aperture. These superleaks are the "guards" which seem to be conducive to observation of intrinsic critical velocities.

We report here a series of pressure head measurements as a function of flow velocity for temperatures between 1.46 and 2.14 K.

3. ANALYSIS

Calculation of the total free energy of an appropriately shaped half-ring pinned to the orifice lip is a difficult problem, but with the aid of some simplifying assumptions, the temperature dependence of the critical velocity may be deduced from this model, and the values of the nucleation theory parameters may be roughly estimated.

The local velocity of superfluid flow as a function of the distance y from a sharp edge with dihedral angle θ is[11]

$$v(y) = v_s A y^{\alpha - 1} \tag{5}$$

where A is a constant, and

$$\alpha = \pi/(2\pi - \theta) \tag{6}$$

The shape of the half-ring attached to the edge can be found by applying the criterion for a critical state: the local self-induced velocity v_0 must everywhere on the ring match the local flow velocity $v(y)$. The geometry of the ring is related to the flow field through the local induction approximation,[14] which states that the self-induced velocity of an element of vortex filament is proportional to its local curvature; that is,

$$v_0 = B/R \tag{7}$$

For a circular ring

$$B = \kappa(\eta - 1/2)/4\pi \tag{8}$$

which is nearly constant; for other shapes, the term involving η is probably slightly different. Applying the condition for a critical state,

$$B/R = v_s A y^{\alpha - 1} \tag{9}$$

Because the assumed local wall geometry has no length scale, the geometry of the ring scales with velocity in such a way that it retains its shape, but only varies in size as v_s changes; so the ratio of radius of curvature at a point to the distance of the point from the edge is a constant. Specifically, for the point farthest from the edge,

$$R(y_0)/y_0(v_s) = C \tag{10}$$

where $y_0(v_s)$ is the maximum value of y, and C is a constant. For a semicircle, $C = 1$; for a flattened half-ring, $C > 1$.

Solving Eqs. (9) and (10) for the size of the half-ring yields

$$y_0(v_s) = (B/CAv_s)^{1/\alpha} \tag{11}$$

Now the activation energy is approximately proportional to the length of line in the critical vortex, which, if the ring maintains its shape as v_s varies, is proportional to the maximum radius of curvature $R(y_0)$. If the energy per unit length of line is ε, and the ratio of line length to maximum radius of curvature is D, then the activation energy is

$$E_a = \varepsilon D R(y_0) = \varepsilon D C y_0 \tag{12}$$

For a circular ring,

$$\varepsilon = (\rho_s \kappa^2/8\pi)(\eta - 5/2) \tag{13}$$

which should also hold for other shapes to logarithmic accuracy. For a circle, of course, $D = 2\pi$; for a flattened half-ring, therefore, $D < \pi$.

Finally, Eq. (11) can be substituted into Eq. (12) and the result written in a form reminiscent of that found for the homogeneous case:

$$E_a(v_s) = \beta'(\rho_s/\rho) v_s^{-1/\alpha} \tag{14}$$

where

$$\beta' = (\rho\varepsilon/\rho_s) DC(B/CA)^{1/\alpha} \tag{15}$$

A convenient approach to analyzing the pressure head data according to this model is to take the logarithm of both sides of Eq. (1). Defining

$$\Gamma = \ln(\rho\kappa V \nu_0) \tag{16}$$

this procedure yields

$$\ln \Delta p = \Gamma - (\beta'/k)(\rho_s/\rho T) v_s^{-1/\alpha} \tag{17}$$

Solving for the velocity,

$$v_s = \left[\frac{\beta'}{k(\Gamma - \ln \Delta p)}\right]^{\alpha} \left(\frac{\rho_s}{\rho T}\right)^{\alpha} \tag{18}$$

Now if the velocity data are plotted on log–log scales against the temperature-dependent quantity $\rho_s/\rho T$, the result should be a family of straight lines, one for each value of Δp, and all with slope α. This plot is shown in Fig. 3. The values of α are far from the homogeneous nucleation value of 1, but close to the value of 0.67 expected for a right-angle orifice lip. The variation of α with Δp is quite small; for purposes of analysis we adopt the value for $\Delta p = 1$ dyne/cm^2, $\alpha = 0.69$.

Having adopted a value for α, we may use Eq. (17) to determine the values of the nucleation prefactor Γ and the activation energy parameter β' from the pressure head dependence of the velocity. Figure 4 shows a plot of $\ln \Delta p$ vs. $(\rho_s/\rho T) v_s^{-1/\alpha}$. The simplified inhomogeneous nucleation model predicts a single line of slope $-\beta'/k$ and intercept Γ. Roughly, at least, that result obtains, with $\beta' = 2.2 \pm 0.5 \times 10^{-11}$ cgs and $\Gamma = 15 \pm 4$ cgs.

Given α, and continuing with the assumption that the critical vortex is not too far from semicircular, the expected value of β' can easily be calculated from Eq. (15), provided that the velocity coefficient A and the core parameter η can first be estimated. An approximate integration of the velocity distribution over the orifice cross section gives a value $A =$

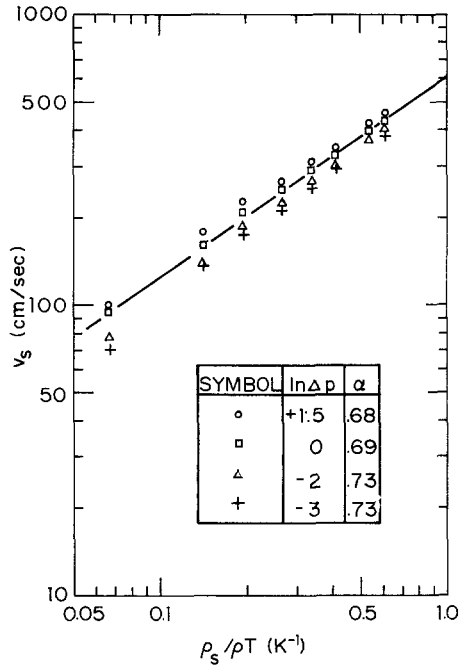

Fig. 3. The temperature dependence of velocity. The solid line is fitted to the $\ln \Delta p = 0$ data. Its slope is $\alpha = 0.69$.

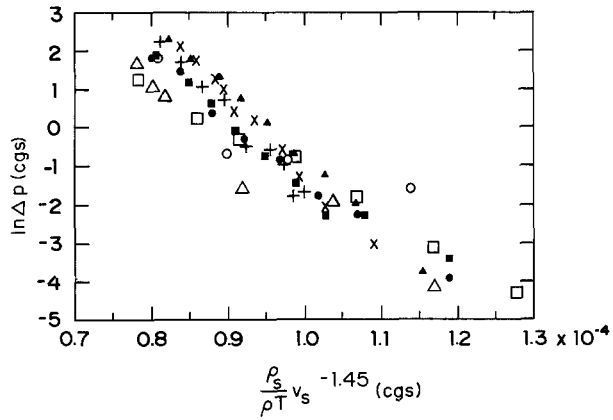

Fig. 4. The pressure head-velocity relation. ×, 1.463 K; +, 1.57 K; ▲, 1.740 K; ■, 1.943 K; △, 2.017 K; □, 2.083 K; ○, 2.141 K. The slope of the aggregate of all points is $\beta'/k = 1.63 \times 10^5$ cgs; the $\ln \Delta p$ intercept is $\Gamma = 14.8$ cgs.

0.054. The vortex parameter η can be found by solving Eq. (4) with R_c from Eqs. (10) and (11). The extremes over the experimental range are 3.1 and 3.6. Finally, for a semicircular ring, Eq. (15) becomes

$$\beta' = \frac{\rho\kappa^2(\eta - 5/2)}{8}\left[\frac{\kappa(\eta - 1/2)}{4\pi A}\right]^{1/\alpha} \tag{19}$$

at 1.94 K, a result of comparable magnitude to the experimental value.

The measured value of Γ is somewhat more difficult to account for. If Γ is calculated from its definition, Eq. (16), naively using the entire channel volume for V, and using 10^{34} Hz/cm^3 for ν_0, the result is about 48, a value much higher than is measured. The measured value of Γ can be accounted for (keeping $\nu_0 = 10^{34}$ Hz/cm^3) only if the nucleation volume is about 10^{-24} cm^3. Now the typical size of a critical ring is, from Eq. (11), on the order of only 10^{-7} cm, so if the nucleation volume is taken to be only a layer of thickness y_0 near the lip, the active surface must be about 10^{-17} cm^2. This tiny area could not be accounted for even if vortex production were dominated by a short section of extra-sharp lip with radius of order 10 Å. This does not deter us from suggesting, however, that such sections may exist, for the straightness of the plots of Eq. (18) strongly suggest an edge-nucleated process. Any edge roundness on the order of the size of the critical ring would cause an upward curvature of those graphs at high v_s, and none is seen.

In order to escape the difficulty of unexpectedly low values of Γ, other workers, notably Campbell *et al.*[15] and Harrison and Mendelssohn,[8] have adjusted the attempt frequency ν_0. A strong temperature dependence is found, with ν_0 falling exponentially as temperature rises. This is qualitatively similar to our results.

A closer look at Fig. 4 reveals the temperature dependences of Γ and β'. When the data are fit for each temperature separately, different values for Γ and β' result, which are given in Table I, together with calculated values of η and β' for the experimental velocities. The measured values of Γ and β' show similar temperature dependence. The calculated values of β' are less temperature dependent and about three times smaller than the measured values.

It is not surprising that the ratio β'/Γ is found to be temperature independent; this is forced by the analysis. Properly, we should return to Eq. (18) and try to redetermine α simultaneously with a temperature-dependent Γ or β'. Since β' depends on reasonably well-understood properties of the quantized vortex, it would be surprising if it had stronger than the logarithmic dependence on v_s and T implied by Eq. (3) or (15) and (4), apart from the uncertainties of the vortex configuration and of the

TABLE I

Comparison of Experimental and Theoretical Values of the Nucleation Parameters[a]

T, K	Γ, cgs	β'(exp) 10^{-11} cgs	η	β'(theor) 10^{-11} cgs
1.463	19.6	2.87	3.43	0.623
1.571	19.9	2.98	3.46	0.654
1.740	17.5	2.53	3.45	0.645
1.854	13.2	1.98	3.35	0.549
1.943	13.3	2.01	3.38	0.577
2.017	11.1	1.77	3.31	0.513
2.083	9.9	1.52	3.28	0.487
2.141	8.0	1.14	3.20	0.419

[a]The values of η are calculated for experimental conditions at $\ln \Delta p = 0$.

temperature dependence of the core radius a. Therefore, to investigate the effect of a temperature-dependent Γ, we will treat β' as a constant. A strong temperature dependence of Γ is also surprising, but cannot be ruled out, as there is no satisfactory theory for ν_0.

The salient experimental fact, including also gravitational flow measurements with similar orifices,[10] is that data for constant Δp plotted as in Fig. 3 always give a straight line. This implies that any temperature dependence of Γ is well represented by the form

$$\Gamma(T) = \Gamma_0(\rho_s/\rho T)^{\delta} \tag{20}$$

with some exponent δ. Then the slope α' measured in Fig. 3 is to be reinterpreted (for $\ln \Delta p \approx 0$) as

$$\alpha' = \alpha(1-\delta) \tag{21}$$

The dependence of velocity on pressure head gives Γ as before. We can obtain a self-consistent fit to the present data with $\alpha = 1.03$, $\delta = 0.33$, $\Gamma_0 = 35$, and $\beta' = 2.4 \times 10^{-12}$ cgs.

To evaluate this fit, we note that Γ varies from 30 at 1.463 K to 14 at 2.141 K, which are closer to the anticipated value. Since $\alpha \approx 1$, which corresponds to a half-ring in a locally uniform flow, the expected value of β' is approximately $\beta/2 \approx 4 \times 10^{-12}$ cgs. This would be reduced if velocity enhancement near the walls were taken into acount, so the fitted value appears reasonable.

4. CONCLUSIONS

We suggest two possible interpretations of these results. The first is that Γ has an intrinsic temperature dependence given by Eq. (20) with

$\delta \approx 0.33$, and vortex nucleation occurs on a relatively flat portion of wall, so there may be a velocity enhancement (say by a factor E), but there is no appreciable velocity gradient on a scale up to the largest critical ring radius $R_{\max}$ for the velocity range studied. Consequently, $\alpha \approx 1$. Nucleation must still occur predominantly in the region of maximum velocity, for which the orifice lip is the primary candidate. For consistency, $R_{\max}$ must be smaller than the radius R_L of the lip. We estimate the enhancement E as a function of R_L as

$$E \approx 0.5(5\ \mu\text{m}/R_L)^{1/3} \tag{22}$$

Combining this with Eqs. (7) and (8), and using the minimum mean velocity of 90 cm/sec, we obtain the condition $R_L > 50$ Å. This is well below the observational constraint. The energy parameter is consistent within the uncertainty of possible corrections to η for small vortices. Therefore this interpretation appears satisfactory, apart from requiring an unexplained strong temperature dependence of Γ.

The alternate interpretation assumes that the temperature dependence of v_s is in fact due to a segment of very sharp edge, and Γ is nearly constant. This is possible if the measured dependence of Δp on velocity does not simply represent independent nucleation of vortices, but that some other process comes into play at finite nucleation rates. The sort of thing required could be temporary pinning of supercritical vortices so as to reduce the local velocity at the nucleation site. If something like this occurs, we have insufficient informaton to extract Γ and β'.

REFERENCES

1. S. V. Iordanskii, *Zh. Eksp. Teor. Fiz.* **48**, 708 (1965) *Sov. Phys.—JETP* **21**, 467 (1965)].
2. J. S. Langer and M. E. Fisher, *Phys. Rev. Lett.* **19**, 560 (1967).
3. J. S. Langer and J. D. Reppy, in *Progress in Low Temperature Physics*, Vol. VI, C. J. Gorter, ed. (North-Holland, Amsterdam, 1970), pp. 1–35.
4. R. J. Donnelly and P. H. Roberts, *Phil. Trans. R. Soc.* **271**, 41 (1971).
5. J. R. Clow and J. D. Reppy, *Phys. Rev. Lett.* **19**, 291 (1967).
6. G. Kukich, R. P. Henkel, and J. D. Reppy, *Phys. Rev. Lett.* **21**, 197 (1968).
7. H. A. Notarys, *Phys. Rev. Lett.* **22**, 1240 (1969).
8. S. J. Harrison and K. Mendelssohn, in *Low Temperature Physics—LT*13, K. D. Timmerhaus, W. J. O'Sullivan, and E. F. Hammel, eds. (Plenum, New York, 1974), Vol. I, p. 298.
9. G. B. Hess, *Phys. Rev. Lett.* **29**, 96 (1972).
10. G. B. Hess, in *Low Temperature Physics—LT* **13**, K. D. Timmerhaus, W. J. O'Sullivan, and E. F. Hammel, eds. (Plenum, New York, 1974), Vol. I, p. 302.
11. Y. J. Brown, Dissertation, University of Virginia (1979).
12. G. van der Heijden, W. J. P. de Voogt, and H. C. Kramers, *Physica* **59**, 473 (1972).
13. B. M. Guenin and G. B. Hess, *Physica* **101B**, 285 (1980).
14. R. J. Arms and F. R. Hama, *Phys. Fluids* **8**, 553 (1965).
15. L. J. Campbell, E. F. Hammel, J. K. Hoffer, and W. E. Keller, *J. Low Temp. Phys.* **24**, 527 (1976).